Elucidation of Anti-ssDNA Autoantibody BV 04-01 Binding Interactions with Homooligonucleotides†

Sergey Y. Tetin,‡ Catherine A. Rumbley,§ Theodore L. Hazlett,‖ and Edward W. Voss, Jr.*,‡

Department of Microbiology, Department of Cell and Structural Biology, and Laboratory of Fluorescence Dynamics, Department of Physics, University of Illinois, Urbana, Illinois 61801

Received April 7, 1993; Revised Manuscript Received June 1, 1993

ABSTRACT: Binding interactions of various synthetic oligohomonucleotides with anti-ssDNA autoantibody BV 04-01 (IgG2b, κ) and the corresponding single-chain antibody (SCA) 04-01/212 were studied. Oligonucleotide binding to IgG or SCA resulted in quenching of the protein's tryptophan fluorescence permitting direct assessment of ligand binding under equilibrium conditions. The effect of oligothymidylate length, $(dT)_n$, on tryptophan quenching was evaluated. The equilibrium dissociation constants (K_d) for the binding of $(dT)_6$ and $(dT)_8$ were the same [$(1.3 \pm 0.02) \times 10^{-7}$ M], while decreasing the length of the oligothymidylate to $(dT)_3$ increased the K_d an order of magnitude. To assess base specificity, the comparative binding of other hexahomonucleotides was examined. Neither $(dA)_6$ nor $(dC)_6$ showed measurable binding, while the dissociation constant for $(dG)_6$ was $(7.1 \pm 0.3) \times 10^{-7}$ M. Fluorescence lifetime quenching data correlated with the steady-state binding results and indicated that the quenching process contains both dynamic and static components. The ability of BV 04-01 to bind $(dT)_6$ and $(dG)_6$ nucleotides was further supported by fluorescence anisotropy studies with fluorescein-labeled hexadeoxynucleotides. Various levels of tryptophan fluorescence quenching upon titration with oligothymidylates of different length, as well as the similar affinities for $(dT)_6$ and $(dG)_6$, supported the concept that the groove-type binding pocket in BV 04-01 consists of binding subsites that cooperatively adapt for efficient binding of oligonucleotides.

The large diversity in primary structures of complementarity-determining regions (CDRs),[1] which form the antigen binding site, is an inherent property of antibodies. Mutual interactions of CDR and framework regions of the polypeptide chain restrict the number of feasible binding site architectures (Padlan & Kabat, 1991). It appears that, on the basis of these interactions, two general diverse structural organizations result: a deep pocket suitable for effective binding of small antigenic determinants or haptens and a relatively long, wide, shallow groove for interaction with extended antigens [reviewed by Kabat et al. (1991)]. The antigen binding site shows a conformational malleability that varies significantly in different antibodies [reviewed by Davies and Padlan (1990)], providing reciprocal adaptation of the antigenic determinant and the binding site. For a given active site, antigen specificity and affinity have evolved from the potential for mutual conformational adaptability in the binding pair. These binding pairs may combine rigid and/or flexible structures.

Anti-DNA antibodies contain an example of a groove-type binding site. Ballard and Voss (1985) generated a panel of murine anti-DNA monoclonal autoantibodies displaying either single-strand (ss) DNA or double-strand (ds) DNA specificity. The variable region primary structures of five monoclonal autoantibodies from that panel were determined (Smith & Voss, 1990). One of the monoclonal antibodies, BV 04-01 (an IgG2b, κ protein), was subsequently crystallized, and the three-dimensional structure resolved a groove-type binding site (Herron et al., 1991) in both the unliganded and liganded forms. Ligand-binding radioimmunoassay-based studies with BV 04-01 showed preferential specificity for single-stranded oligonucleotides, especially oligothymidylate (Smith et al., 1989). To characterize the role of specific amino acids in the binding site of BV 04-01 in interactions with thymidine oligonucleotides, single-chain antibody (SCA) and mutants were constructed (Rumbley et al., 1993).

To understand the specificity and affinity of BV 04-01 for oligonucleotides, a quantitative assay for equilibrium binding parameters, which covers many orders in antigen concentration, is required. Such an assay, based on the high sensitivity and accuracy of intrinsic fluorescence from tryptophan residues in antibodies, monitors antigen-induced (based on titrations) fluorescence quenching (Velick et al., 1960; Eisen, 1964). With modern fluorescence instrumentation, this protein–ligand assay can measure a range of dissociation constants (K_d) from 10^{-10} to 10^{-4} M (Weber, 1992). We applied this concept of antibody fluorescence quenching to quantitatively reexamine the oligonucleotide binding specificity of BV 04-01. Our results confirm the BV 04-01 specificity for oligo(thymidylic acid) and absence of binding for oligodeoxyadenylate or oligodeoxycytidylate (Smith et al., 1989). The unexpectedly high affinity of BV 04-01 for oligodeoxyguanylate prompted us to employ a fluorescence anisotropy assay, using fluorescein-labeled oligonucleotides. The fluorescence anisotropy experiments also demonstrated comparable affinities of $(dT)_6$ and $(dG)_6$ for BV 04-01. The RIA (Smith et al., 1989) and crystallographic studies (Herron et al., 1991) with BV 04-01 suggest that, at least for oligothymidylate, chain length is an

† This work was supported by a grant from the Biotechnology Research Development Corp., Peoria, IL. C.A.R. was supported by an NIH Cell and Molecular Biology training grant. The LFD is supported by the National Center for Research Resources of the National Institutes of Health (RR03155) and by UIUC.

* Address correspondence to this author at the Department of Microbiology, University of Illinois, 131 Burrill Hall, 407 S. Goodwin Ave., Urbana, IL 61801.

‡ Department of Microbiology.

§ Department of Cell and Structural Biology.

‖ Department of Physics.

[1] Abbreviations: CDR, complementarity-determining region; Dnp, 2,4-dinitrophenyl; Fl, fluorescein; F_V, 25-kDa fragment of the Ig molecule containing the V_L and V_H domains; HPLC, high-pressure liquid chromatography; Ig, immunoglobulin; $(dT)_n$, polythymidylate; Q_{max}, maximum percent fluorescence quenching; RIA, radioimmunoassay; SCA, single-chain antibody equivalent to the F_V fragment with a 212 polylinker.

0006-2960/93/0432-9011$04.00/0

important factor in determining antigen binding. The fluorescence quenching assay permitted measurements evaluating the effect of oligonucleotide chain length on the equilibrium binding constant.

The quantitative methods for determining equilibrium binding constants and antibody specificity described in this paper also provide information about conformational changes in the anti-DNA antibody, as reflected in tryptophan quenching. This approach will be useful in understanding the whole class of anti-DNA immunoglobulins and representative autoantibodies. Biomedical interest in autoantibodies arises from their pathogenic involvement in human systemic lupus erythematosus (SLE) or the SLE-like syndrome in inbred strains of autoimmune mice [reviewed by Voss (1988)].

MATERIALS AND METHODS

Proteins. The hybridoma cell line BV 04-01 was generated by Ballard et al. (1985), and the anti-ssDNA mouse monoclonal antibody (IgG2b, κ) was obtained from ascites fluid. Ascites fluid was delipified with dextran sulfate and the γ-globulin fraction precipitated in 50% saturated ammonium sulfate. The precipitate was dissolved and dialyzed against 0.1 M potassium phosphate buffer (pH 7.6) prior to incubation (affinity chromatography) with a ssDNA–agarose adsorbent (GIBCO–BRL) equilibrated in the same buffer. Mab BV 04-01 was eluted with 1 M NaCl in 0.1 M potassium phosphate buffer solution, pH 7.6.

The single-chain derivative of BV 04-01 containing the V_L and V_H domains from the BV 04-01 molecule, tethered by a 14 amino acid residue linker (212 polylinker), was constructed, expressed, and folded as previously described (Rumbley et al., 1993). After refolding, SCA was dialyzed against 0.1 M phosphate buffer with 0.15 M NaCl, pH 8.0, and affinity-purified using ssDNA–agarose. The purity of all BV 04-01 proteins was confirmed by SDS–polyacrylamide gel electrophoresis with appropriate molecular weight markers (Laemmli, 1970; Rumbley et al., 1993).

Protein concentration was calculated from absorption spectra at 240–350 nm, corrected for light scattering (Levine & Federici, 1982). Spectra were obtained using a Perkin-Elmer Lambda 5 dual-beam spectrophotometer. The extinction coefficients ($A_{278}^{mg/mL}$) 1.40 and 1.70 for IgG 04-01 and SCA, respectively, were calculated from the chromophore content (Mach et al., 1992) on the basis of the primary structure (Smith & Voss, 1990).

Oligodeoxynucleotide Ligands. The unlabeled oligonucleotides hexathymidylate [$(dT)_6$-5′-OH] and trithymidylates [$(dT)_3$-5′-OH and $(dT)_3$-5′-phosphate] were synthesized by the phosphoramidite method (Beaucage & Caruthers, 1981) and purified by HPLC (University of Illinois Genetic Engineering Facility). All ligands possessed greater than 99% purity by analytical HPLC. Heptathymidylate [$(dT)_7$-5′-OH] and hexathymidylate [$(dT)_6$-5′-OH] were obtained from Sigma (St. Louis, MO) for comparison purposes. No detectable differences in results were observed when $(dT)_6$-5′-OH was compared from either source. All oligonucleotides demonstrated the UV absorption spectra in the region of 240–330 nm, characteristic of nucleotide homopolymers (Voet et al., 1963).

The molar extinction coefficient $\epsilon_\lambda^{(dX)_n}$ for each oligonucleotide was calculated by multiplying the molar coefficient ϵ_λ^X for the corresponding mononucleotide at wavelength λ by the number of monomers (n) in the oligonucleotide. All primary values of ϵ_λ^X were taken from Voet et al. (1963). The following extinction coefficients were calculated: $\epsilon_{265}^{(dT)_3} = 2.85 \times 10^4$ M^{-1} cm^{-1}; $\epsilon_{265}^{(dT)_6} = 5.7 \times 10^4$ M^{-1} cm^{-1}; $\epsilon_{265}^{(dT)_8} = 7.6 \times 10^4$ M^{-1} cm^{-1}; $\epsilon_{252}^{(dG)_6} = 8.1 \times 10^4$ M^{-1} cm^{-1}; $\epsilon_{258}^{(dA)_6} = 9.0 \times 10^4$ M^{-1} cm^{-1}; $\epsilon_{263}^{(dC)_6} = 5.58 \times 10^4$ M^{-1} cm^{-1}.

All fluorescein-labeled oligonucleotides were synthesized and purified by HPLC (Clontech Laboratories, CA). The equal molar concentration of oligonucleotide and fluorescein in each sample was verified by absorption at 240–330 nm (for nucleotides) and 400–560 nm (for fluorescein). A molar extinction coefficient $\epsilon_{490} = 7.2 \times 10^4$ M^{-1} cm^{-1} was used for fluorescein.

Fluorescence Measurements. (A) Steady State. Emission spectra were obtained using an ISS Greg PC photon-counting spectrofluorometer (ISS, Champaign, IL) equipped with prism polarizers. Emission spectra of protein intrinsic fluorescence were recorded in the region of 315–460 nm upon excitation at 295 nm. Excitation and emission band-passes were 8 and 16 nm, respectively. To minimize inner filter effects, the total sample absorption (protein and ligand) was kept below 0.1 OD at 295 nm. An exception was made with $(dT)_3$-5′-OH and $(pG)_6$ studies when the absorption at 295 nm for the samples of highest ligand concentration was in range of 0.3 OD. In these cases the inner filter corrections were made, as described (Parker, 1968). Anisotropy studies with fluorescein-labeled nucleotides were performed using excitation at 480 nm (band-pass 4 nm) and the emission observed at 520 nm (band-pass 4 nm). All measurements were performed at room temperature (approximately 22 °C). Background subtraction, integration of the emission spectra, and collection of anisotropy data were performed using the ISS Greg PC software (ISS, Champaign, IL).

(B) Time Resolved. Fluorescence lifetimes and dynamic polarization data were obtained using a custom-built multifrequency phase and modulation fluorometer based on the Gratton design (Gratton, 1983). Excitation of antibody tryptophan residues was achieved by tuning the output of a mode-locked ND:YAG (Coherent Antares Model 76) pumped, cavity dumped rhodamine dye laser (Coherent Model 700) to 590 nm doubling (Spectra-Physics Model 390 frequency doubler) to 295 nm. Fluorescence emission was monitored through a Schott WG 335-nm cutoff filter and a 340-nm broad band-pass filter. The eliminate polarization artifacts in the lifetime measurements, the excitation beam was routinely polarized normal to the laboratory plane, 0°, and emission was observed at the magic angle, 55°.

Data analysis was performed using either the ISS software package (ISS, Champaign, IL) or the Globals Unlimited Software (Laboratory for Fluorescence Dynamics, Department of Physics, University of Illinois, Urbana, IL).

Curve Fitting. Antibody binding data were analyzed under the assumption that each IgG molecule contains two equivalent, noninteracting binding sites. Data were fit using a simple single binding site model:

$$f(x) = \frac{m[\mathrm{ABS}]_f}{K_d + [\mathrm{ABS}]_f} + c$$

where $f(x)$ is the quenching (Q) or anisotropy being observed, m is the limit of Q_{max} or anisotropy at saturation, K_d is the dissociation constant, $[ABS]_f$ is the concentration of free antibody binding sites, and c is the constant equal to the observed parameter in the absence of ligand (quenching) or antibody (anisotropy). Experimental data were fit to the above equation using the Levinson–Marquardt method in either DeltaGraph Professional (DeltaPoint, Monterey, CA) or Nfit (Island Products, Galveston, TX). The concentration of binding sites and K_d were calculated from the total concen-

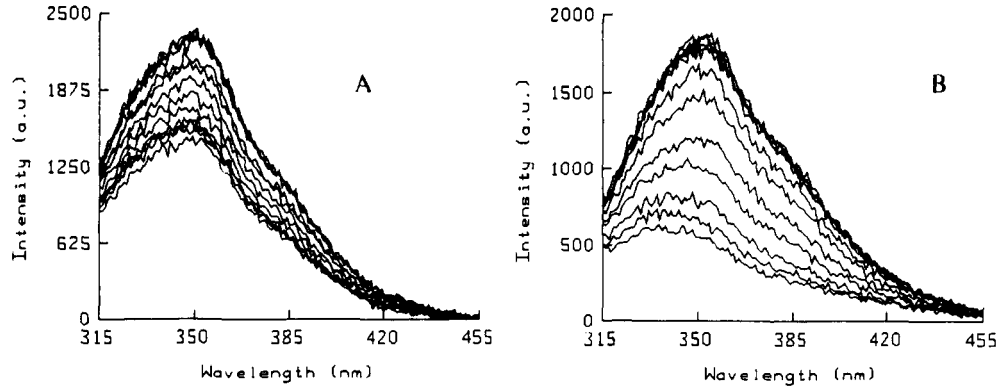

FIGURE 1: Fluorescence spectra of IgG 04-01 (A) and SCA 04-01/212 (B) under titration by the $(dT)_6$ ligand. Excitation was at 295 nm and the bandwidth was 8 nm. The measurements were performed at 22 °C in 0.1 M phosphate buffer, pH 7.6. Corresponding binding plots are presented in Figures 2 and 3.

Table I: Distribution of Tryptophan Residues in Autoantibody BV 04-01

Ig protein	no. of tryptophans
IgG	24
F_C	8
Fab	8
F_V, V_H	4
F_V, V_L	1
SCA	5

tration using repeated estimates of K_d and recalculations of $[ABS]_f$ until the change in estimated K_d was under 1%. The reported errors derive from the correlation matrix in the final fitting.

RESULTS

Tryptophan Content and Fluorescence of BV 04-01. The distribution of tryptophan residues in the IgG 04-01 molecule and subunits is shown in Table I. It is important to note that ten tryptophan residues are located in the two variable portions (five per F_V fragment or SCA derivative) of the BV 04-01 antibody molecule. Since most protein fluorescence originates from excited tryptophan residues, they serve as intrinsic markers which are sensitive to the microenvironment. Velick et al. (1960) used ligand-dependent quenching of antibody fluorescence as an indicator of binding in affinity determinations describing rabbit antibodies specific for 2,4-dinitrophenyl. Lee et al. (1982) estimated the binding constants of autoantibody HEd 10 with polynucleotides on the basis of intrinsic protein fluorescence quenching upon ligand binding. We have utilized a similar quenching effect in the study of oligonucleotide binding to the anti-ssDNA autoantibody BV 04-01. The observed ligand-induced quenching coupled with the high sensitivity of fluorescence spectroscopy has permitted investigations of oligonucleotide binding at protein and ligand concentrations between 10^{-8} and 10^{-7} M (range of expected dissociation constants) for the accurate determination of relevant binding parameters.

Intrinsic fluorescence spectra of IgG 04-01 and SCA 04-01/212 upon titration of the $(dT)_6$ oligodeoxynucleotide are shown in Figure 1. The observed ligand-dependent quenching was found to be more pronounced in SCA (Figure 1B) than in the intact IgG (Figure 1A). Indeed, the fact that Q_{max} for SCA, an IgG 04-01 variable domain construct (Rumbley et al., 1993), was approximately 70% (Figure 3 and Table II) supports localization of quenched tryptophan residues in the binding portion of BV 04-01. The K_d values (Table II) of SCA and parent IgG differ by 1 order of magnitude, which

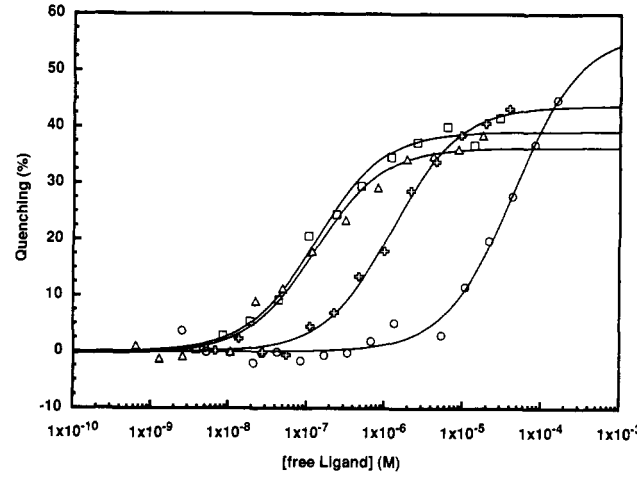

FIGURE 2: Binding plots of thymidine oligonucleotides and IgG 04-01. Quenching of protein fluorescence is shown as a function of free oligonucleotide concentration. All measurements were performed at 22 °C in 0.1 M phosphate buffer, pH 7.6. Total concentrations of antigen binding sites (ABS) for $(dT)_3$-5′-OH (○), $(dT)_3$-5′-phosphate (cross), $(dT)_6$ (△), and $(dT)_8$ (□) were 5.3×10^{-7}, $5,7 \times 10^{-7}$, 3.9×10^{-7}, and 2.9×10^{-7} M, respectively.

indicates absence of stabilization effects normally contributed by the constant domains. In addition to fluorescence quenching, the ligand–antibody complex also displayed an apparent blue shift relative to the unliganded form, an effect attributed to emission from unquenched, buried tryptophan residues. Areas under the emission curves at each step in the titration were used to establish ligand binding data and were subsequently fit to a simple, single binding site model as described in Materials and Methods.

Comparison of Polythymidines. Figure 2 and Table II show the binding of IgG 04-01 with $(dT)_8$, $(dT)_6$, and $(dT)_3$ nucleotides. The affinity and quenching of the 04-01 protein for the larger oligomeric nucleotides, $(dT)_8$ and $(dT)_6$, were the same within experimental error. In contrast, the dissociation constant for the trinucleotide, $(dT)_3$-5′-phosphate, was higher by 1 order of magnitude, and the level of tryptophan fluorescence quenching at saturation increased by 7%. Removal of the 5′-phosphate group from the ligand led to a further increase in the dissociation constant by 35-fold (i.e., a decrease in the affinity) and an additional 13% increase in quenching.

Fluorescence Lifetime Quenching Data. To better understand the origin and mechanism of the quenching of tryptophan fluorescence induced by oligonucleotide binding in BV 04-01 protein fluorescence, lifetime quenching data of SCA were

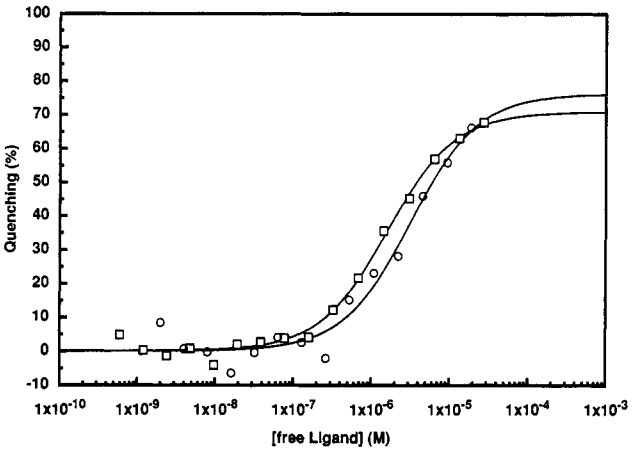

FIGURE 3: Binding plots of thymidine oligonucleotides and SCA 04-01/212. Quenching of protein fluorescence is shown as a function of free oligonucleotide concentration. All measurements were performed at 22 °C in 0.1 M phosphate buffer, pH 7.6. The total concentration of antigen binding sites (ABS) was 7.0×10^{-7} M for both $(dT)_8$ (□) and $(dT)_6$ (○).

Table II: Quenching of Intrinsic Protein Fluorescence and Dissociation Constants of BV 04-01 and Deoxypolynucleotide Ligands

ligand	Q_{max} (%)	K_d (μM)	ΔG (kcal/M) (association)
	IgG 04-01		
$(dT)_3$-5′-OH	56.9 ± 3.7	44.2 ± 7.6	−5.8 ± 0.1
$(dT)_3$-5′-phosphate	43.8 ± 1.0	1.25 ± 0.13	−7.9 ± 0.1
$(dT)_6$-5′-OH	36.7 ± 0.2	0.13 ± 0.02	−9.3 ± 0.1
$(dT)_8$-5′-OH	39.2 ± 1.4	0.13 ± 0.02	−9.3 ± 0.1
$(dG)_6$-5′-OH	22.7 ± 2.2	0.71 ± 0.31	−8.2 ± 0.3
$(dA)_6$-5′-OH		>100	
$(dC)_6$-5′-OH		>100	
	SCA 04-01/212		
$(dT)_6$-5′-OH	76.3 ± 6.5	3.21 ± 0.89	−7.4 ± 0.2
$(dT)_8$-5′-OH	70.9 ± 1.9	1.60 ± 0.17	−7.8 ± 0.1

obtained through titration of $(dT)_6$. Fluorescence lifetime results were best fit with a three-component decay model. Fluorescence intensity average lifetime, defined as $\sum(f_i \times \tau_i)$, was plotted as a function of the free ligand concentration and fit, assuming a single site binding model, with a $K_d = (6.9 \pm 3.1) \times 10^{-6}$ M and a lifetime $Q_{max} = 45.4 \pm 7.9\%$. Dissociation constants resolved from the intensity and lifetime data were the same within experimental error, while the maximal fluorescence intensity quenching was greater. The fluorescence lifetime data reflect dynamic quenching while both dynamic and static quenching processes are monitored by the quenching of fluorescence emission. These results suggest that the quenching effect is due to both dynamic and static processes.

Homodeoxynucleotide Specificity. The base specificity exhibited by antibody BV 04-01 was examined with the homooligonucleotides $(dG)_6$, $(dA)_6$, and $(dC)_6$, and the results are shown in Figure 4 and Table II. At concentrations ranging from 10^{-9} to 10^{-4} M, neither $(dA)_6$ nor $(dC)_6$ was found to quench the IgG 04-01 tryptophan fluorescence. However, $(dG)_6$ induced measurable quenching of 22.7 ± 2.2%, from which a dissociation constant of $(7.1 \pm 3.1) \times 10^{-7}$ M was calculated (Figure 4, Table II). This result is close to binding constants determined for $(dT)_6$. The observation of $(dG)_6$ binding was inconsistent with radioimmunoassays which did not detect binding of oligodeoxyguanylic acid by BV 04-01 (Smith et al., 1989).

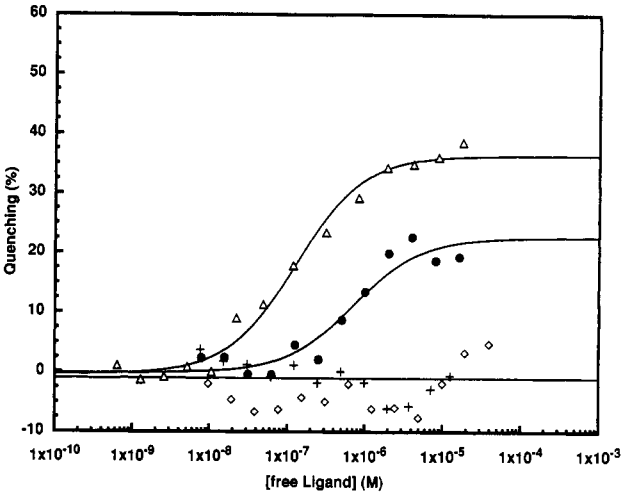

FIGURE 4: Binding plots of different oligohomonucleotides and IgG 04-01. Quenching of protein fluorescence is shown as a function of free oligonucleotide concentration. All measurements were performed at 22 °C in 0.1 M phosphate buffer, pH 7.6. Total concentrations of antigen binding sites (ABS) for $(dT)_6$ (△), $(dG)_6$ (●), $(dA)_6$ (◇), and $(dC)_6$ (+) were 3.9×10^{-7}, 4.3×10^{-7}, 5.6×10^{-7}, and 4.9×10^{-7} M, respectively.

Anisotropy Studies. To further explore the results and interpretations based on the tryptophan quenching experiments, a fluorescence anisotropy binding assay was developed. The assay was based on increased anisotropy shown by fluorescein-labeled oligonucleotides upon binding to IgG BV 04-01 antibodies. Increased anisotropy reflects the hindered motion of the bound probe. The fluorescence spectra of the free and bound probes were identical. In the absence of fluorescence intensity changes, the sample anisotropy is proportional to the relative concentrations of the free and bound ligand. Thus, the anisotropy data can be used to accurately monitor immune complex formation. Fluorescein is a suitable fluorescent probe in such studies due to its high quantum yield (0.92) and excitation coefficient ($\epsilon_{490} = 7.2 \times 10^4$ M^{-1} cm^{-1}), which permits dilution of the fluorescein-labeled compound in the range of the expressed dissociation constants. Results of titrations of fluorescein-labeled oligodeoxynucleotides by IgG 04-01 are shown in Figure 5 and Table III. To avoid possible influence of the fluorescein label on the binding process, oligonucleotides of one or two bases longer than necessary for efficient binding, as determined by the tryptophan quenching studies, were used. Both oligothymidylate ligands $(dT)_8$-5′-Fl and $(dT)_7$-5′-Fl demonstrated the same affinity and anisotropy in the presence of saturating levels of protein binding sites. The anisotropy for the $(dG)_7$-5′-Fl–antibody complex was lower than that observed for the interaction with oligothymidine nucleotides, while the K_d value differed only by a factor of 2. Oligodeoxyadenylate and oligodeoxycytidylate exhibited no changes in anisotropy throughout titration of antibodies over the entire concentration range tested. It is noteworthy that all fluorescein-labeled ligands demonstrated a 4–10-fold lower affinity in fluorescence anisotropy studies than unlabeled polynucleotides, as measured in the fluorescence quenching assay.

DISCUSSION

Since anti-DNA autoantibodies act as pathogenic markers in SLE, their specificity and affinity have been extensively studied [see Koffler et al. (1971) and Munns and Freeman (1989) and reviews by Tan (1982), Stollar (1986), and Voss (1988)]. Our research is targeted at understanding the anti-

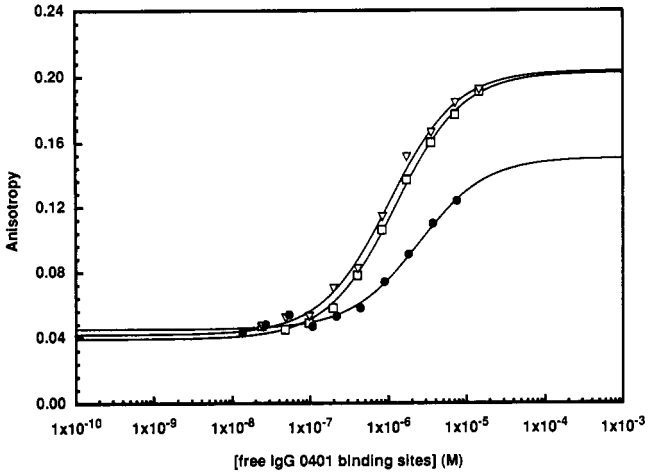

FIGURE 5: Binding plots of fluorescein-labeled oligonucleotides and IgG 04-01. Anisotropy of labeled ligands is shown as a function of free IgG binding site concentration. All measurements were performed at 22 °C in 0.1 M phosphate buffer, pH 7.6. Concentrations of $(dT)_8$-5′-Fl (□), $(dT)_7$-5′-Fl (▽), and $(dG)_7$-5′-Fl (●) are 3.0×10^{-7}, 2.4×10^{-7}, and 3.9×10^{-7} M, respectively. Data for $(dA)_7$-5′-Fl and $(dC)_7$-5′-Fl are not shown. IgG 04-01 did not change the anisotropy of these ligands at any of the concentrations measured.

Table III: Fluorescence Anisotropy of Fluorescein-Labeled Deoxypolynucleotides and Their Dissociation Constants with IgG 04-01

ligand	anisotropy (at saturation)	K_d (μM)	ΔG (kcal/M) (association)
$(dT)_7$-5′-Fl	0.204 ± 0.005	1.09 ± 0.15	−8.0 ± 0.06
$(dT)_8$-5′-Fl	0.203 ± 0.003	1.25 ± 0.09	−7.9 ± 0.04
$(dG)_7$-5′-Fl	0.150 ± 0.007	2.47 ± 0.49	−7.5 ± 0.12
$(dA)_7$-5′-Fl	0.042 ± 0.002	>100	
$(dC)_7$-5′-Fl	0.042 ± 0.002	>100	

ssDNA antibody binding site organization and its capacity to accommodate various oligonucleotide ligands.

Analytical methods based on the fluorescence properties of proteins or labeled DNA ligands can provide valuable information about equilibrium binding constants (i.e., thermodynamics), specificity, and mechanism of antibody–DNA interactions. The solution-phase tryptophan quenching assay used in this study was modified on the basis of the assay introduced by Velick et al. (1960) and Eisen (1964) for anti-DNP antibodies. They attributed the efficient quenching of tryptophan fluorescence with DNP titration to energy transfer from the fluorescent antibody to the nonfluorescent bound hapten. Such an energy-transfer mechanism is not applicable to the DNA–antibody reaction because tryptophan emission does not overlap the absorption spectra of nucleotides. We propose another mechanism for the quenching effect observed in our experiments, namely, the microenvironment of certain tryptophan residues in the antibody changes upon ligand binding, and this change is reflected in a quenched fluorescence spectrum.

There are 24 tryptophan residues in the IgG BV 04-01 molecule, with 8 in each Fab fragment and 8 in the F_C fragment. The variable domains (V_H,V_L) of each F_V fragment, which are modeled by SCA, contain 5 tryptophans (Table I). When the level of IgG and SCA fluorescence quenching induced by $(dT)_6$ (Figure 1, Table II) was compared, a 2-fold higher efficiency in quenching of SCA was measured even though the parent molecule contains 14 additional tryptophan residues distributed throughout the constant regions (F_C; C_H1 and C_L domains of Fab). Clearly, these additional residues are normally quenched and do not contribute significantly to the overall fluorescence of IgG. On the basis of this comparison, the majority of BV 04-01 fluorescence can be attributed to the remaining 5 tryptophan residues in the two F_V fragments.

Analysis of the three-dimensional structure of BV 04-01 Fab fragments reveals that the five tryptophans located in the variable domains (V_L and V_H) (Table I) do not contribute equivalently to the protein's fluorescence. Two of the tryptophans, Trp 36H and Trp 35L, are within a radius of less than 6 Å from disulfide bonds in the corresponding heavy and light domains and thus are expected to be highly quenched (Cowgill, 1970; Harris & Hudson, 1991).

The microenvironment of Trp 100aH, which is directly involved in interactions with ssDNA, changes significantly in the liganded complex. Examination of the crystal structure of BV 04-01 Fab unliganded and bound with $(dT)_3$-5′-phosphate (Herron et al., 1991) shows that the charged groups of the ligand move close to the indole moiety of Trp 100aH (Figure 6). In addition, several significant displacements of the polypeptide chain are apparent and result in a triple stacking interaction with the middle thymine base sandwiched between Tyr 32L and Trp 100aH. For these reasons Trp 100aH is a strong candidate for quenching upon ligand binding (Harris & Hudson, 1991). However, the overall fluorescence quenching of BV 04-01 upon ligand binding cannot be assigned to this single tryptophan residue. In site-specific mutagenesis studies Rumbley et al. (1993) showed that the replacement of Trp 100aH by phenylalanine or tyrosine still yielded measurable quenching of antibody fluorescence upon thymidine nucleotide binding.

The two remaining tryptophans are Trp 47H and Trp 103H. Trp 47H is located relatively distant from the binding groove on the intradomain surface, while Trp 103H is closer to the groove. The microenvironments of Trp 103H and Trp 47H contain several polar groups. From crystallographic analysis the microenvironments of both tryptophans, Trp 103H and Trp 47H, are displaced upon $(dT)_3$ binding. These displacements include changes in the orientation of the polar groups relative to the indole rings and should affect the fluorescence spectra (Harris & Hudson, 1991). On the basis of this structural analysis, the origin of tryptophan quenching in BV 04-01 results primarily from direct interactions of the ssDNA ligands with tryptophan residue 100aH. Indirect interactions, due to the conformational transition induced by antigen binding, probably quench Trp 103H and Trp 47H fluorescence to a lesser degree.

In fluorescence quenching studies, intensity changes reflect both dynamic and static mechanisms of quenching, whereas changes in fluorescence lifetime exclusively delineate a dynamic, diffusion-based, mechanism [see review by Eftink (1991)]. On the basis of fluorescence lifetime data, the quenching of the tryptophan residues in SCA by titration with $(dT)_6$ yields a lower efficiency for the dynamic quenching mechanism (Q_{max} = 45%), as compared with fluorescence intensity quenching (Q_{max} = 70%). The difference in fluorescence quenching efficiency measured by lifetime and steady-state intensity arises from a significant static component in BV 04-01 quenching. Our structural analysis, based on crystallographic data, suggests that the triple stacking of Trp 100aH with the thymine base in the thymidine oligonucleotides and Tyr 32L may account for this static quenching component.

Herron et al. (1991) resolved the three-dimensional structure for the complex of Fab 04-01 with $(dT)_3$-5′-phosphate. The importance of the 5′-terminal phosphate group in trithymidylate binding was noted in our $(dT)_3$-5′-phosphate and $(dT)_3$-

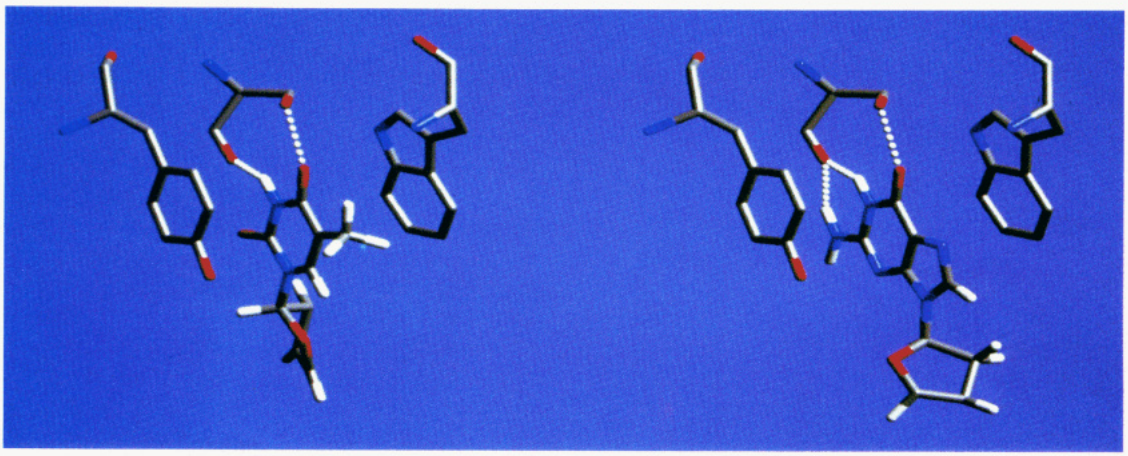

FIGURE 6: Model of the BV 04-01 nucleotide base binding site provided for the Fab 04-01 and $(dT)_3$-5′-phosphate complex (Herron et al., 1991). The thymine base (left panel) inserts between Tyr 32L and Trp 100aH. Involved in hydrogen bonding (white dots) are the thymine 4 carbonyl oxygen with the Ser 91L side chain and the thymine N_3 hydrogen with the carbonyl oxygen of the main polypeptide chain at the Ser 91L. The hypothetical replacement of thymine by guanine is shown in the right panel. Guanine replaces thymine without distortion of the protein groups involved in stacking interactions or hydrogen bonding. Guanine groups at positions 1, 6, and 2 are hydrogen bonded with groups of Ser 91L. The orientation of the sugar–phosphate backbone (low on the picture) is significantly changed in the deoxyguanosine nucleotide.

5′-OH studies. The presence of the 5′-phosphate group decreases the dissociation constant 35-fold, which in terms of free energy amounts to −2.1 kcal/M. The additional free energy supplied by the phosphate group derives from the 2 hydrogen bonds and 14 van der Waals contacts reported for the 5′-phosphate in the crystallographic studies (Herron et al., 1991). Loss of these bonds in the $(dT)_3$-5′-OH–antibody complex is expected to change the free energy more significantly than the 2.1 kcal/M observed. Such a discrepancy may be explained by a reorientation of the dephosphorylated ligand within the binding groove, increasing the number of interactions or strength of the remaining bonds. The interpretation is supported by the measurable increase in ligand-dependent quenching from 44% to 57% for $(dT)_3$-5′-OH (Table II).

Among the nucleotides examined, only oligodeoxyguanylate and oligothymidylates show significant affinity for IgG 04-01 (Table II). The K_d for $(dG)_6$ is about 5-fold higher than for $(dT)_6$, with a free energy loss of about 1 kcal/M. This finding is inconsistent with previously published data (Smith et al., 1989) and suggestions from crystallographic modeling (Herron et al., 1991). Further support for deoxyguanosine oligonucleotides binding to BV 04-01 comes from studies of fluorescein-labeled nucleotides (Table III). BV 04-01 binds both oligonucleotides, $(dT)_7$-5′-Fl and $(dG)_7$-5′-Fl, with a slight decrease in affinity of the latter (<0.4 kcal/M). The reduced anisotropy of $(dG)_7$-5′-Fl at saturation indicates a greater rotational motion in its complex with BV 04-01. Furthermore, the level of tryptophan quenching is lower for $(dG)_6$ than for $(dT)_6$, indicating a different conformation of the BV 04-01 binding groove arising from the size and structure of the guanine base. Decreased Q_{max} and anisotropy values observed with oligodeoxyguanylate are compatible with this model.

The ball-and-stick model of the middle thymine base in the Fab BV 04-01 and $(dT)_3$-5′-phosphate complex is shown in Figure 6 (left panel). The model design is based on the atomic coordinates (Herron, personal communication) by analogy with the model published previously (Herron et al., 1991). The hypothetical interactions of the guanine base in the same environment of the binding site are shown in the right panel of Figure 6. The guanine replaces thymine in this model without any apparent distortion of the protein groups involved in stacking interactions or hydrogen bond formation. Clearly, the hydrogen bonds formed by the hydrogen atom of nitrogen 3 and oxygen 4 of the thymine base can be equivalently formed by the guanine groups in positions 1 and 6. The third hydrogen bond formed by the amino group attached to carbon 2 of guanine should further stabilize the complex. The pentameric ring of guanine is outside of the triple stack. Of course, the larger size of guanine alters the interaction of the homonucleotide's sugar–phosphate backbone with the binding groove of BV 04-01.

Increasing the length of thymidine oligonucleotide from a trimer, $(dT)_3$-5′-OH or $(dT)_3$-5′-phosphate, to a hexamer dramatically decreased the K_d (Table II). The statistically significant decrease in intrinsic protein fluorescence (Q_{max}) with $(dT)_3$-5′-phosphate or with $(dT)_3$-5′-OH, as compared with $(dT)_6$, suggests that the hexamer adopts an orientation different from that of the trimers in the BV 04-01 binding groove. Further, increasing the length of the oligothymidylate ligand to a heptamer does not change the binding constant or the level of tryptophan quenching. These results are consistent with previous radioimmunoassay data which showed no changes in binding properties of thymidine oligonucleotides longer than a pentamer (Smith et al., 1989). The binding groove dimensions of the BV 04-01 antibody, based on crystallographic analysis (Herron et al., 1991), are compatible with the accommodation of oligonucleotides of 5–6 monomers in length. The enhanced binding of oligothymidylates longer than 4–5 monomers was also found in another monoclonal anti-ssDNA autoantibody, HEd 10 (Lee et al., 1982) and in polyclonal autoantibodies from human SLE serum (Stollar et al., 1962).

Our results, pertaining to nucleotide size, chain length, and base specificity, demonstrate that quantifiable fluorescence quenching occurs due to changes in the microenvironment of the previously discussed tryptophans. The pronounced but shallow binding groove in BV 04-01 may be subdivided into several regions (subsites) characterized by different levels of contact with the ssDNA ligands. An unequal distribution of interactions with each nucleotide was shown for the $(dT)_3$-5′-phosphate ligand in the crystallographic studies (Herron et al., 1991). Each discrete subsite possesses specificity for portions of the repetitive structure of ssDNA. For example, the subsite formed by Trp 100aH and Tyr 32L is specific for a particular structural portion of thymine or guanine (Figure

6), which does not exist in adenine or cytosine. Other subsites are specific for phosphate groups, deoxyribose moieties, or other bases. Collectively, these subsites are expected to exhibit cooperativity of antigen binding, such as a "microavidity" effect.

The concept of binding groove subsite heterogeneity introduces the possibility of frame shifts in the binding of polynucleotides, especially homopolynucleotides. Our data support the equivalence of frame-shifted homonucleotide positions upon binding of hexameric or longer ligands. For the trimer, the terminal nucleotides may assume various orientations upon binding. The observed decrease in affinity of 5′-end-labeled oligonucleotides reflects such a microheterogeneity in binding (Table III). The induced-fit mode of interaction in BV 04-01 complexes observed by Herron et al. (1991) and Stevens et al. (1993) supports this concept. The high conformational heterogeneity of the binding groove may cause difficulties in preparation of immunochemical reagents such as monoclonal anti-idiotypic antibodies (Voss et al., 1992).

In summary, the various levels of tryptophan fluorescence quenching upon titration with thymidine oligonucleotide of different lengths, as well as the similar affinities for $(dT)_6$ and $(dG)_6$, support the concept that the groove-type binding pocket in BV 04-01 consists of binding subsites that cooperatively adapt for efficient binding of polynucleotides.

ACKNOWLEDGMENT

We express our gratitude to Gregorio Weber, W. W. Mantulin, A. H.-J. Wang, and H. H. Robinson for their insight and helpful discussion. The fluorescence measurements were performed at the Laboratory for Fluorescence Dynamics (LFD) at the University of Illinois at Urbana–Champaign.

REFERENCES

Ballard, D. W., & Voss, E. W., Jr. (1985) *J. Immunol. 135*, 3372–3380.

Beaucage, S. L., & Caruthers, M. H. (1981) *Tetrahedron Lett. 22*, 1859–1862.

Cowgill, R. W. (1970) *Biochim. Biophys. Acta 207*, 556–559.

Davies, R. R., & Padlan, E. A. (1990) *Annu. Rev. Biochem. 59*, 439–473.

Eftink, M. R. (1991) in *Topics in Fluorescence Spectroscopy* (Lakowitz, J. R., Ed.) Vol. 2, pp 53–120, Plenum Press, New York and London.

Eisen, H. N. (1964) in *Methods in Medical Research* (Eisen, H. N., Ed.) Vol. 10, pp 115–121, Year Book Medical Publishers, Chicago, IL.

Gratton, E., & Limkeman, M. (1983) *Biophys. J. 44*, 315–324.

Harris, D. L., & Hudson, B. S. (1991) *Chem. Phys. 158*, 353–582.

Herron, J. N., He, X.-M., Gibson, A. L., Ballard, D. W., Blier, P., Pace, P., Bothwell, A., Voss, E. W., Jr., & Edmundson, A. B. (1991) *Proteins 11*, 159–175.

Kabat, E. A., Wu, T. T., Perry, H. M., Gottesman, K. S., & Foeller, C. (1991) *Sequences of Proteins of Immunological Interest*, Vol. 1, U.S. Department of Health and Human Services, NIH, Bethesda, MD.

Koffler, D., Carr, R., Agnello, V., Thoburn, R., & Kunkel, H. G. (1971) *J. Exp. Med. 134*, 294–312.

Laemmli, U. K. (1970) *Nature 227*, 680–685.

Lee, J. S., Dombroski, D. F., & Mosman, T. R. (1982) *Biochemistry 21*, 4940–4945.

Levine, R. L., & Federici, M. M. (1982) *Biochemistry 21*, 2600–2606.

Mach, H., Middaugh, C. R., & Lewis, R. V. (1992) *Anal. Biochem. 200*, 74–80.

Munns, T. W., & Freeman, S. K. (1989) *Biochemistry 28*, 10048–10054.

Padlan, E., & Kabat, E. (1991) *Methods Enzymol. 203*, 3–21.

Parker, C. A. (1968) *Photoluminescence of Solutions*, pp 220–226, Elsevier, Amsterdam.

Rumbley, C. A., Denzin, L. K., Yantz, L., Tetin, S. Y., & Voss, E. W., Jr. (1993) *J. Biol. Chem. 268*, 13667–13674.

Smith, R. G., & Voss, E. W., Jr. (1990) *Mol. Immunol. 27*, 463–470.

Smith, R. G., Ballard, D. W., Blier, P. R., Pace, P. E., Bothwell, A., Herron, J. N., Edmundson, A. B., & Voss, E. W., Jr. (1989) *J. Indian Inst. Sci. 69*, 25–46.

Stevens, S. Y., Swanson, P. C., Voss, E. W., Jr., & Glick, G. D. (1993) *J. Am. Chem. Soc. 115*, 1585–1586.

Stollar, B. D. (1986) *CRC Crit. Rev. Biochem. 20*, 1–36.

Stollar, B. D., Levine, L., Lehrer, H. I., & Van Vunakis, H. (1962) *Proc. Natl. Acad. Sci. U.S.A. 48*, 847–880.

Tan, E. M. (1982) *Adv. Immunol. 32*, 167–240.

Velick, S. F., Parker, C. W., & Eisen, H. N. (1960) *Proc. Natl. Acad. Sci. U.S.A. 46*, 1470–1482.

Voet, D., Gratzer, W. B., Cox, R. A., & Doty, P. (1963) *Biopolymers 1*, 193–208.

Voss, E. W., Jr. (1988) *Anti-DNA Antibodies in SLE*, CRC Press, Boca Raton, FL.

Voss, E. W., Jr., Weidner, K. M., & Denzin, L. K. (1992) *Immunol. Invest. 21*, 71–83.

Weber, G. (1992) *Protein Interaction*, Routledge, Chapman & Hall, New York and London.